Mathl Comput. Modelling, Vol. 14, pp. 231–236, 1990
Printed in Great Britain

0895-7177/90 $3.00 + 0.00
Pergamon Press plc

CALIBRATION AND STOCHASTIC MODELING OF A LASER-GYRO FOR LABORATORY TESTING.

J. Aranda*, J.M. de la Cruz*, H. Ruiperez**, S. Dormido*

* Dpto. Informatica y Automatica. Facultad de Ciencias. UNED. 28040-Madrid. Spain

** CESELSA. Alcobendas. Madrid. Spain.

ABSTRACT.-

The paper describe laboratory test procedures and the methology for calibration and stochastic modeling of inertial sensor, with application to the laser-gyro.

The calibration consists in the parameter estimation for deterministic modeling of the sensor. By using a three axes test table, it's shown, that a rate test positive and negative from each one of the axes of the table is enought to estimate the model's parameters.

The stochastic model is obtained with two different techniques: by a description of in-run drift and by Time Series Analysis (TSA).

INTRODUCTION.-

This paper presents the methodology, laboratoy test procedures and technics for calibration and stochastic modeling of a laser-gyro.

The laser-gyro used is a Ferranti´s ring laser gyro (RLG) type 160-200-002.

The RLG is an unconventional gyro which is particularly well matched to the strapdown enviroment. The theory for operation of this device has been detailed in the literature [1-4].

Theoretically the laser gyro is an ideal single-degree-of-freedom floated gyro, with errors associated with mass properties removed.

The laser-gyro model is:

$$\frac{N}{\Delta t} = (S_o + S(\omega_{in}))\ \omega_{in} + D \qquad (1)$$

where:

N : number pulses in the Δt time.
Δt : period of lectures of pulses.
S_o : nominal scale factor.
$S(\omega_{in})$: scale factor error (no-linearities) function of ω_{in} (multiplicative error).
ω_{in} : input angular rate.
D : drift error (aditive error).

$$D = D_F + D_T + \omega_r$$

where: D_F = "fixed" drift error.
D_T = Switch-on transients.
ω_r = random bias error.

Part of these errors are deterministic and predictable and hence are calibrated and compensated. Other errors are random noise that can not be compensated, but if accurate models are obtained from test data, then it is possible design a Kalman filter to compensate for some of these errors.

The calibration consists in the parameter estimations for deterministic error model of the gyro. The used technique is a modification of the Joos and Krogman tecnique [5] applied to the laser-gyro.

The stocastic model for random drift is obtained with two different techniques: from a description of in-run drift and from Time Series Analysis [6].

CALIBRATION.-

The methodology for calibration is summarized in the following steps:

1.- Definition of the gyro´s model from literature and previous tests.
2.- Definition of the kind tests than can be applied to the gyro.
3.- Assembly of the tests in the laboratory.
4.- Record of the gyro output for each test.
5.- With the previous record, the model´s parameters are identificated and estimated.

The gyro model is the deterministic part of model (1).

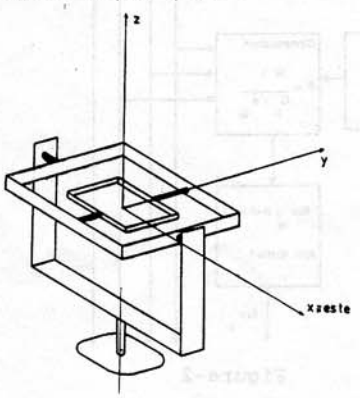

Figure-1

The gyro is mounted on a three axes test table (figure-1). The tests are rate-test and multiposition static test. The temperature and ambient conditions are constant for each test. The coordinate frames for the problem (the local frame and the gimbal frame) are defined:

- local frame {E,N,U}: orthogonal frame from local East, North and Up.
- gimbal frame $\{g_x, g_y, g_z\}$: orthogonal frame tie to the inside gimbal. g_y is

about inside axis of the table.

In the gimbal frame the input axis of the gyro is defined by three cosines ($\delta_x, \delta_y, \delta_z$). The input rate is:

$$\omega_{in} = \delta_x\omega_x + \delta_y\omega_y + \delta_z\omega_z \qquad (2)$$

where $\omega_x, \omega_y, \omega_z$ are the rate in the gimbal frame.

The objetive of the calibration is to determine: the nominal scale factor (S_o), the fixed drift (D_F), the cosines ($\delta_x, \delta_y, \delta_z$), and the parameters of the scale factor errors $S(\omega_{in})$.

This parameters are determined for different temperatures, so the tests are repeted for diferent temperatures.

The procedure (figure 2) consist of two parts. In the first part, the fixed drift, the cosines and a value for scale factor are estimated. In the second part the scale factor $S(\omega_{in})$ is identified by a function of the input rate.

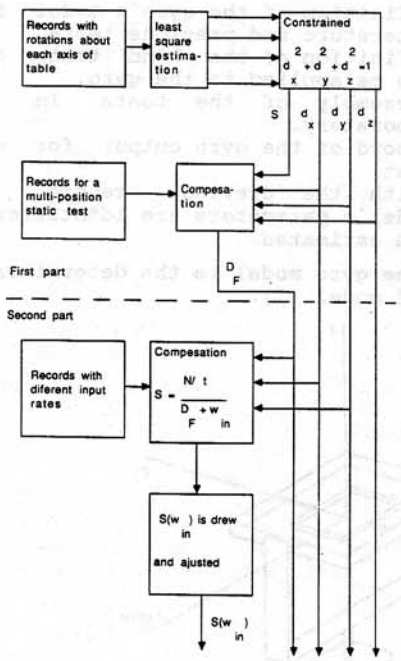

Figure-2

Estimation of the cosines and the fixed drift.-

The test-table is adjusted in a position where the gimbal frame coincide with the local frame. In this position the table is rotated in CW and CCW about each axe. In order to consider the same scale factor the tests are performed with a constant absolute value input rate.

The parameters $S\delta_x$, $S\delta_y$, $S\delta_z$, SD_F are determined in a least square sense applying linear regression techniques by the equation:

$$\frac{N}{\Delta t} = (S\delta_x)\omega_x + (S\delta_y)\omega_y + (S\delta_z)\omega_z + (SD_F) \qquad (3)$$

where:

- N : number of pulses of the gyro for a period of axis rotation.
- Δt : period of the axis rotation.
- S : nominal scale factor.
- $\delta_x, \delta_y, \delta_z$: cosines.
- D_F : fixed drift
- $\omega_x, \omega_y, \omega_z$: rate about each table axis in gimbal frame.

We use the constrained:

$$\delta_x^2 + \delta_y^2 + \delta_z^2 = 1 \qquad (4)$$

And then we can estimate $S, D_F, \delta_x, \delta_y, \delta_z$ by:

$$S = \sqrt{(S\delta_x)^2 + (S\delta_y)^2 + (S\delta_z)^2}$$

$$D_F = (SD_F)/S$$

$$\delta_x = (S\delta_x)/S$$

$$\delta_y = (S\delta_y)/S$$

$$\delta_z = (S\delta_z)/S$$

Table-1 has the result for a simulated laser-gyro.

Parameter	Value	95% confidence interval	
$S D_F$	0.38411	0.38398	0.38926
$S\delta_x$	46331.42	46331.42	46331.42
$S\delta_y$	46331.41	46331.41	46331.42
$S\delta_z$	113488.3	113488.3	113488.3
RSS = 0.527 E-3		RMS = 0.2637 E-3	
Covariance matrix			
0.3485 E-5	0.9498 E-7	0.1348 E-6	0.8098 E-6
0.025816	0.3884 E-5	0.3673 E-8	0.2207 E-7
0.378816	0.97797 E-3	0.3632 E-5	0.3132 E-7
0.16806	0.43388 E-2	0.6366519 E-2	0.6662 E-5
Correlation matrix			

Estimate value	optimist σ	pessimist σ
$\hat{S}$ = 131045	σ_S = 0.00355	σ_S = 0.00376
$\hat{\delta}_x$ = 0.3535535	σ_{δ_x} = 4.89475 E-9	σ_{δ_x} = 2.51833 E-8
$\hat{\delta}_y$ = 0.3535534	σ_{δ_y} = 4.39892 E-9	σ_{δ_y} = 2.46875 E-8
$\hat{\delta}_z$ = 0.8660254	σ_{δ_z} = 5.1517 E-9	σ_{δ_z} = 4.4545 E-8
$\hat{D}_F$ = 0.293117 E-5	σ_{D_F} = 1.4245 E-8	σ_{D_F} = 1.42451 E-8

Table-1

If it is used the Marquard non-linear estimation procedure with the table-1 values as initial values but without the constrained (4) then the final values of the non-linear procedure are more distant of the real values than the initial values. If it is used the constrained (4) in the non-linear procedure then it is not finded a trend of search and the final values of the procedure are the initial values.

The fixed drift is reestimated by a multi-position static test. The test-table is oriented in a number of pre-determined positions. The measure gyro are compensated for the scale factor and the cosines. The fixed drift is calculated for each position by:

$$D_F = \frac{N/\Delta t}{S} - (\delta_x \omega_x + \delta_y \omega_y + \delta_z \omega_z + D_F) \qquad (5)$$

where $\omega_x, \omega_y, \omega_z$: is the earth rate in gimbal frame.

The final estimate of D_F is obtained by averaging of the fixed drift calculate for every position.

Identification of the scale factor.-

In order to detemine possible non-linearities of the scale factor, tests are performed at various rotation rates of the test-table.

For each rate the scale factor is calculated by

$$S = \frac{N/\Delta t}{D_F + \omega_{in}} \qquad (6)$$

where ω_{in} is the gyro input rate.

The scale factor versus the input rate is drew and adjusted.

The figure-3 show the scale-factor for the simulated laser-gyro of the table-1.

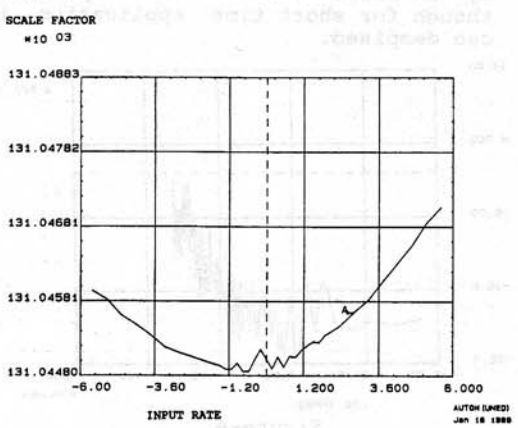

Figure-3

METHODS OF DESCRIBING THE IN-RUN DRIFT.-

The steps to follow for describing the in-run drift are:

- Data acquisition and conversion into a form suitable for further processing.
- Preprocessing:
  - Qualitative analysis: test for stationarity and randomness.
  - DC component and trend removal.
  - Calculation of statistical parameters.
  - Time plots (description of the switch-on transients).
- Data analysis:
  - Spectral analysis (description by spectral density plots).
  - Covariance analysis (description by autocorrelation functions).
  - Standard desviation versus time analysis (description by sigma plot).

Data acquisition:

The gyro is fixed on a test-table with constant temperature and ambient conditions.

For the laser gyro the output is in the form of pulses, each pulse representing a fixed angular increment. These pulses are fed to an up-down counter, wich is reset (and its output stored) at fixed time intervals.

The output is recorded on a magnetic tape as a series numbers, each number representing an angle increment over a fixed period of time.

The sample time must be small enough to enable the detection of the maximum frequecy of interes, but not smaller.

Preprocessing:

The stationarity of the record data gyro is tested with the run test [7].

The randomness is analysed in the time domain by inspection of the frequency histograms of the data records. To investigate the randomness of the data, the χ^2 (goodness of fit) test has been executed on the data [7].

The mean value, standard deviation and average slope are calculated. Then, the measured data are filtered by the following algoritm [5] (removal of DC component and linear trend):

$$x_i = v_i - \bar{v} - \bar{\alpha}\,(i - N/2)\,\Delta t \qquad (7)$$

with Δt the sampling interval, $\bar{v}$ the mean value, $\bar{\alpha}$ the average slope, N the number of data and $\{v_i\}_{i=0}^{N-1}$ the record data.

Description of the switch-on transients (time plots):

The plot of the angular rate error (or angular error) is a useful way, and indeed the only way, of observing the switch-on transients. Switch-on transients occur with different time constants.

Graphs for different sampling time are made. Each of these graphs is estudied, to decide whether any of them shows a switch-on transient, and to decide by inspection, what form of function best fits the transient.

Afterwards the approximate parameters of the function are determined.

Power Spectral Density and autocorrelation function:

Two appoaches to further quatifying the variability of sensor drift rate are the autocorrelation function (ACF) and its associated power spectral density (PSD) [8].

The ACF, $R_{xx}(\tau)$, directly indicates the time domain variability of the drift term.

The PSD, a frequency domain characterization of the drift, is the Fourier transform G(f) to $R_{xx}(\tau)$.

The PSD data presented in this paper makes use of the Hamming window.

Standard deviation vesus time plots:

This is the method of descibing random drift which is most frequently of greatest value to the user.

A very good rigorous treatment is descibed by Sargent and Wyman [9], and examples for diferent gyros are found in many articles [10-12].

The procedure consist in computing the standard deviation ($\sigma^2(t)$) of data for different sample time. The relationship with PSD is:

$$\sigma^2(t) = 4 \int_0^\infty \frac{G(f)\ (1-\cos 2\pi f t)}{(2\pi f)^2}\, dt \qquad (8)$$

CHARACTERISATION OF RLG IN-RUN DRIFT.-

By the above techniques, the random noise of the Ferranti´s RLG type 160-200*002, having a scale factor of 1.574 sec/pulse, has been characterized.

The gyro is assembly on a test-table with the input axes vertical. The sense rate is:

$$\omega_i = \Omega \sin L \qquad (9)$$

with:
Ω: Earth´s rate = 15 sec/sec.
L: Latitude = 40°32´51´´ (Latitude of Madrid).

Table 2 show statistical values for a typical record with a sample time of 1 second and 15 hours runs. It is noticed a little ramp with a slope about 10^{-7}, what it´s discarded in short time application.

Mean Value	6.344 pulses
Standard deviation	0.539 pulses
Average slope	-0.18E-6 pul/seg

Table-2

The study of time plots does not show switch-on transients.

Figures 4,5 and 6 shows PSD, ACF and σ-plot for this record. The noise observed are:

- A rate white noise (angle random walk) of 0.22 pulses/$sec^{1/2}$ = 0.0059°/$hr^{1/2}$. It correspondes to the $T^{-1/2}$ slope segment of σ-plot and f^0 slope segment of PSD plot. It is the error in the beat frequency caused by the dither rate going into and out of lock-in with random phase.
- Angle quantization. It results from resetting an integrator each time its output reaches a preset value $\pm\Delta\theta$. The root mean square (rms) angle value is $\Delta\theta/\sqrt{6}$, since these is quatization uncertainty both at the beginning and at the end of each quantization period. Dither spillover also contribute to the quantization effect. If the output quantization is $\Delta\theta$ and the root mean square spillover is σ_{sp}, the effect is the same as a quantization of $\sqrt{\Delta\theta^2+\sigma_{sp}^2}$. It correspondes to the T^{-1} slope segment of σ-plot and the f^2 slope segment of PSD. If the total quantization is 1.29 pulses, and the quantization is 1 pulse then the rms spillover is 0.82 pulses = 1.29 sec.
- A pink rate noise. It correspondes to the end segment of σ-plot with T^0 slope. For this error we cannot postulate a mechanism but it has been observed in practical measurement on various gyro types. It can be modeled by a first order Markov process, though for short time application it can despised.

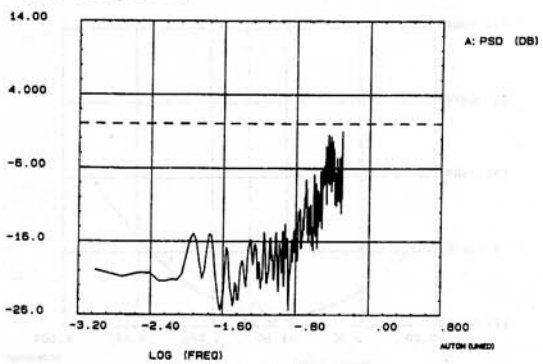

Figure-4

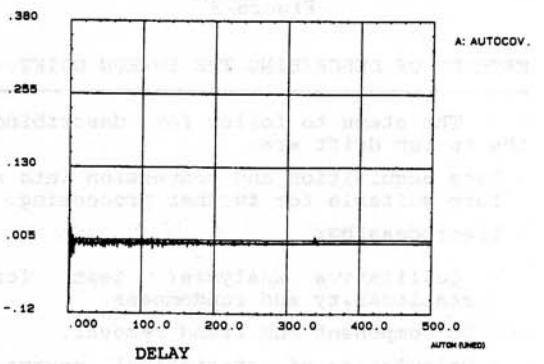

Figure-5

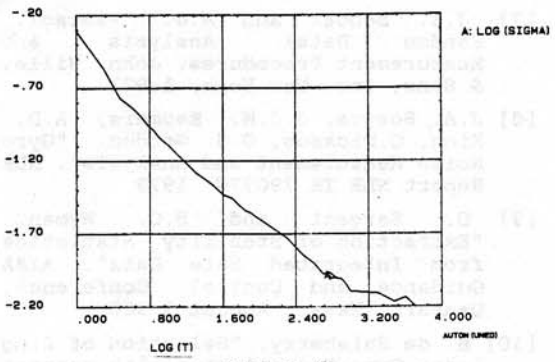

Figure-6

DRIFT MODEL OF THE RLG.-

The gyro drift is assumed to be a linear combination of a random bias, a rate white noise, a random ramp and a fist-order Markov process (pink rate noise). This is shown in block diagram in figure 7. The available measurements are the angular increments corrupted by a noise sequence.

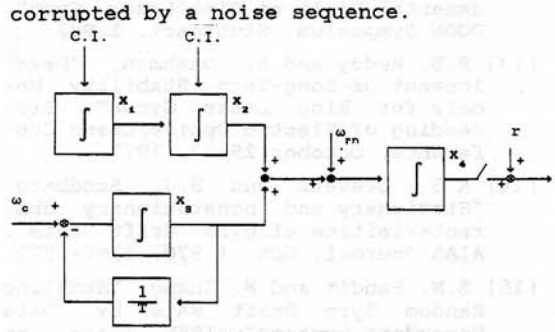

Figure-7

The system can be represented in the form:

$$\dot{x}_1 = 0 \qquad \text{Slope's ramp}$$

$$\dot{x}_2 = x_1 \qquad \text{Bias + ramp}$$

$$\dot{x}_3 = -1/T\, x_3 + \omega_c \qquad \text{Pink rate noise} \qquad (10)$$

$$\dot{x}_4 = x_2 + x_3 + \omega_{rn}$$

$$z(t) = x_4(t) + r(t)$$

where: $\omega_{rn}(\cdot,\cdot)$ is the rate white noise, and $r(\cdot,\cdot)$ is the quantization uncertainty.

The measurement in angular increments assume a reset of x_4. In each sample period x_4 is setted to $x_4 - z$.

The value of the rate ramp and the pink rate noise are small. For many apllication the model is reduced to be a linear combination of random bias and a rate white noise (figure 8).

The shaping filter is reduced to:

$$\dot{x}_1 = 0$$

$$\dot{x}_2 = x_1 + \omega_{rn} \qquad (11)$$

$$z(t) = x_2(t) + r(t)$$

with the same reset for the last integrator.

The difference betwen the two models is minimized by lightly adjusting the process noise.

These models are validated by simulation and test in Kalman filters.

Figure 9 shows a σ-plot for a simulation of model (10), and figure 10 show σ-plot for model (11). The difference is a little ramp at end of the σ-plot.

It is shown that for short-time application the model (11) is enough. The rate ramp and the pink rate noise are evident in long-time, and they are despised in short-time application.

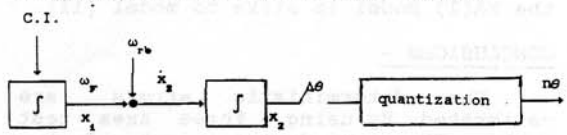

Figure-8

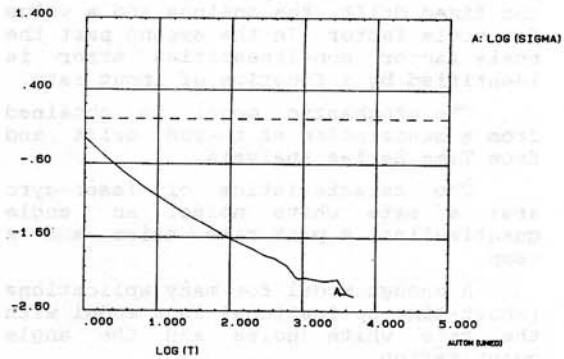

Figure-9

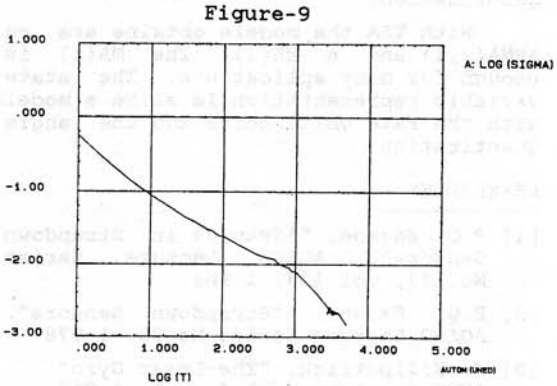

Figure-10

MODELING BY TSA.-

The Time Series Analysis approach consist of: 1) identification of the model structure, 2) estimation of the model parameters, and 3) diagnostic checking of the residuals for white Gaussian noise properties. These procedures are described in [13-15].

Table 3 show the models for a record with a sample time of 1 second.

$$z_k = \phi_1 z_{k-1} + \phi_2 z_{k-2} + a_k - \theta_1 a_{k-1}$$

	ϕ_1	ϕ_2	θ_1	α	σ^2
MA(1)	-	-	0.436	0.096	0.223
ARMA(2,1)	-0.381	-0.146	0.0543	0.253	0.222

Table-3

The ARMA(2,1) model needs five or six state variables for a shaping filter. Futher, the ARMA(2,1) model is not better that the MA(1) model in a lot of applications.

A state variable representation of the MA(1) model is alike to model (11).

CONCLUSIONS.-

The deterministic errors are calibrated. By using a three axes test table. The procedure consist of two parts. In the first part are estimated the fixed drift, the cosines and a value for scale factor. In the second part the scale factor non-linearities error is identified by a function of input rate.

The stochastic model is obtained from a description of in-run drift and from Time Series Analysis.

The caracteristics of laser-gyro are: a rate white noise, an angle quantization, a pink rate noise and a ramp.

A enough model for many aplications (short-time aplications) is a model with the rate white noise and the angle quantization.

With TSA the models obtaine are on ARMA(2,1) and a MA(1). The MA(1) is enough for many aplications. The state variable representation is alike a model with the rate white noise and the angle quantization.

REFERENCES.-

[1] P.G. Savage. "Advances in Strapdown Sensors". AGARD Lecture Series No.133, vol 133, 1.984.

[2] P.G. Savage. "Strapdown Sensors". AGARD Lecture Series No.95, 1.978

[3] J. Killpatrick. "The Laser Gyro" IEEE Spectrum, vol.4, oct. 1.967,

[4] F. Aronowitz. "The Laser Gyro". Laser Applications, vol.1, edited by M. Ross, Academic Press, 1.971.

[5] D.K. Joos and U.K. Krogmann. "Identification and Determination of Strapdown Error-Parameters by Laboratory Testing". AGARDograph No. 254. April 1981.

[6] G.E.P. Box and G.M. Jenkinks. "Time Series Analysis: forecasting and control". Holdan-Day. 1976. Revised edition.

[7] J.S. Bendat and A.G. Piersol. Random Data: Analysis and Measurement Procedures. John Willey & Sons, Inc. New York, 1.971

[8] J.A. Bosgra, J.J.M. Reomers, A.D. King, G.Dickson, G.S. Gordon. "Gyro Noise Measurement and Analysis". NLR Report NLR TR 79077U, 1979

[9] D. Sargent and B.O. Wyman. "Extraction of Stability Statistics from Integrated Rate Data". AIAA Guidance and Control Conference, Danvers, Mass., August 1.980

[10] B. de Salaberry. "Selection of Ring Laser Gyro Technologies with respect to Specific Applications". AGARD Short Course on Optical Gyro. Stuttgart 1982

[11] S.W. Hammons and V.J. Ashby. "Mechanically Dithered RLG at Quantum Limit". NAECON Proceeding, 1.981

[12] T. Callaghan, S. Callaghan, J. House, C. Tettemer, F.Aronowitz. "Fundamental Limit of Ring Laser Gyro". DGON Symposium, Stuttgart, 1.982

[13] P.B. Reddy and A. Dushman. "Development of Long-Term Stability Models for Ring Laser Gyros". Proceeding of Electro Optics/Laser Conference. October 25-27, 1977.

[14] A.S. Oravetz and H.J. Sandberg. "Stationary and nonstationary characterisitics of gyro drift rate". AIAA Journal, Oct. 1.970, 1766-1772

[15] S.M. Pandit and W. Zhang. "Modeling Random Gyro Drift Rate by Data Dependent Systems". IEEE Trans. on Aerospace and Electronics Systems, vol. AES-22, no. 4, July 1.986.